

Surface Heat Fluxes from the NCEP/NCAR and NCEP/DOE Reanalyses at the KEO Buoy Site

Masahisa Kubota¹, Noriyasu Iwabe¹, Meghan F. Cronin²,
and Hiroyuki Tomita³

¹School of Marine Science and Technology, Tokai University, Shimizu, Shizuoka, Japan

²Pacific Marine Environmental Laboratory, NOAA, Seattle, Washington, USA

³Institute of Observational Research for Global Change, Japan Agency for Marine and Earth Science Technology,
Yokosuka, Japan

Correspondence: kubota@mercury.oi.u-tokai.ac.jp

1. INTRODUCTION

Global ocean surface flux provided by reanalysis is widely used for various studies because of their long and consistent time series, and homogeneous spatial resolution. Popular reanalysis products include, for example, the 40-year European Centre for Medium-Range weather Forecasts (ECMWF) reanalysis (ERA40), the National Centers for Environmental Prediction-National Center for Atmospheric Research (NCEP-NCAR) reanalysis NRA1 [Kalnay et al., 1996], and the NCEP-Department of Energy (DOE) reanalysis NRA2 [Kanamitsu et al. 2000]. Global ocean surface flux data constructed from satellite data, such as the Japanese Ocean Flux data sets with Use of Remote sensing Observations (J-OFURO) [Kubota et al., 2002] and Goddard Satellite-based Surface Turbulent Fluxes (GSSTF) [Chou et al., 2003], are also becoming more widely used. To gain confidence in these products, quantitative comparisons against independent data sets within a variety of different regions are required.

Moore and Renfrew [2002] assessed NRA1 and ERA15 surface turbulent heat flux over the western boundary currents of the North Atlantic and North Pacific Oceans. They found NRA1 surface turbulent heat flux contain significant systematic errors in these regions, with somewhat poorer agreement in the Kuroshio region than in the Gulf Stream region. In June 2004, the Kuroshio Extension Observatory (KEO) buoy was deployed in the Kuroshio Extension recirculation gyre at 144.6°E, 32.4°N to monitor air-sea heat, moisture and momentum fluxes, and upper ocean temperature and salinity. The purpose of this paper is to use data from the first deployment year of the KEO surface buoy to assess the NRA1 and NRA2 heat fluxes in the Kuroshio Extension recirculation gyre.

2. DATA

The KEO buoy is essentially an enhanced Tropical Atmosphere and Ocean (TAO) buoy [e.g., McPhaden et al., 1998; Cronin et al., 2006] modified for the severe conditions of the Kuroshio Extension region. In particular, in order to measure and survive the strong winds in this region, wind velocity at 4 m height was measured with a Väisälä Ultrasonic WS425 during the first deployment (June 2004–May 2005) and a Gill WindSonic anemometer during the second deployment (June 2005–November 2005). Winds are sampled at 2-hz and averaged for 2 minutes every 10 minutes at 4-m altitude. All other sensors were similar to those described by Cronin et al. [2006a]. In particular, in addition to winds, the KEO buoy measured solar and longwave radiation at 2-minute intervals, rain rate at 1-minute intervals at 3.5-m altitude, and air temperature, relative humidity, and surface and subsurface temperature and salinity at 10-minute intervals at 3-m altitude. Details of all sensor specifications and sampling strategies can be found on the KEO webpage: <http://www.pmel.noaa.gov/keo/>. Latent heat flux (LHF) and sensible heat flux (SHF) were computed from the high-resolution (10 minute) SST and surface meteorological measurements using the Coupled Ocean-Atmosphere Response Experiment (COARE) bulk algorithm (Version 3.0) [Fairall et al., 2003].

Net solar radiation (SWR) was computed by reducing the measured downward solar radiation (DSWR) by a factor of $(a-1)$, where a , the albedo at the ocean surface, is set as International Satellite Cloud Climatology Project (ISCCP) climatological monthly mean values (http://isccp.giss.nasa.gov/projects/browse_fc.html). The albedo varies from 0.06 in summer to more than 0.1 in winter. Our sign convention for vertical heat fluxes is that a positive value represents heat loss by the ocean and gained by the atmosphere. Thus the total heat flux (THF) out of the ocean can be represented as:

$$\text{THF} = (a-1)\text{DSWR} + \varepsilon (\sigma T_s^4 - \text{DLWR}) + \text{LHF} + \text{SHF} \quad (1)$$

where the first term on the RHS is the net solar radiation out of the surface (SWR), the second term is the net longwave radiation out of the surface (LWR), and LHF and SHF are the latent and sensible heat losses. Daily-averages of each flux in NRA1 and NRA2 were computed from the 4-times-per day analyses. NRA data, with T62 spatial resolution (about 210 km), are linearly interpolated to the location of the KEO buoy using the four grid points surrounding the KEO buoy.

3. COMPARISON OF HEAT FLUX DATA

3-1. Shortwave radiation flux (SWR)

The daily-mean net shortwave radiation flux observed by the KEO buoy and the differences between the KEO and reanalysis fluxes are shown in Figure 1, with positive values indicating a heat transfer from the ocean to the atmosphere. Shortwave radiation shows remarkable seasonal variability, both in its absolute value and its synoptic variability. The maximum absolute value is about 350 W/m^2 in summer and 125 W/m^2 in winter, while the minimum value is about 25 W/m^2 in both winter and summer. As shown in the NRA and KEO difference plot (Fig. 1), the reanalyses consistently underestimate the amplitude of these events, reflecting the present capability of typhoon prediction with these numerical weather prediction models. The underestimation in summer leads to overestimation of heat flux from the ocean to the atmosphere. Overall, the NRA1 and NRA2 net shortwave radiation (SWR) RMS error is large, 48 and 38 W/m^2 , but the bias is relatively small, -1 and 5 W/m^2 , respectively (Table 1).

Table 1. Statistics for each surface flux component. (a) NRA1 and (b) NRA2

(a)						(b)					
NRA1	SWR	LWR	LHF	SHF	THF	NRA2	SWR	LWR	LHF	SHF	THF
Corr.	0.80	0.79	0.92	0.93	0.93	Corr.	0.88	0.78	0.91	0.94	0.94
RMS.						RMS.					
Error	48	15	48	20	77	Error	38	15	62	23	85
Bias	-1	1	38	9	49	Bias	5	-6	60	7	56

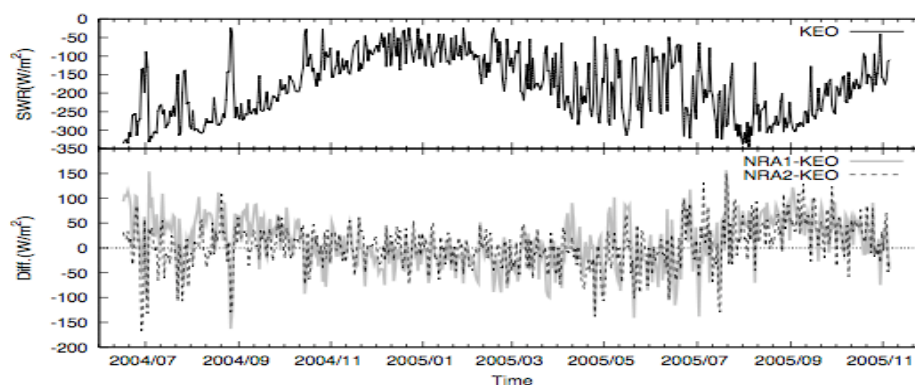


Figure 1. Daily-averaged time series of the net solar radiation (SWR) and the differences between KEO and NRA

3-2. Longwave radiation flux (LWR)

Figure 2 shows time variation of the daily-mean net longwave radiation (LWR) observed by KEO and the differences between KEO and reanalysis fluxes. LWR shows weak seasonal variability. During summer, the differences between the NRA and KEO LWR are relatively small. On the other hand, during winter, net LWR is overestimated by NRA1 and strongly underestimated by NRA2 in comparison to KEO values. The errors in net longwave radiation are primarily due to errors in the downward longwave radiation (DLWR). NRA2 DLWR shows an overestimation in winter of $30\text{-}40\text{W/m}^2$, not found for NRA1. The difference between NRA1 and NRA2 is expected to be related to NRA2 Total Cloud Cover (TCC) errors which appear to be large during this period.

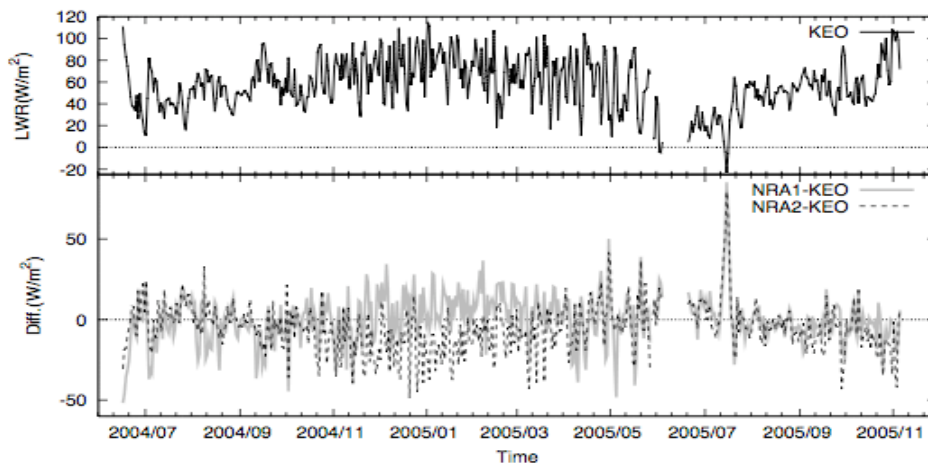


Figure 2. Same as Fig.1, except for the net longwave radiation (LWR).

3-3. Turbulent heat fluxes

Time variation of KEO turbulent heat flux is shown in Fig. 3. Both latent and sensible heat fluxes have extremely large seasonal variations, with large fluxes in winter and small fluxes in summer, as expected. LHF is nearly always larger than SHF and reached more than 400 W/m^2 in winter. SHF however is not insignificant. In winter, SHF is sometimes more than 100W/m^2 .

Both reanalyses overestimated latent heat flux in comparison to KEO, with the overestimation being larger for NRA2 than for NRA1 (Table 1). The LHF bias is 39 W/m^2 for NRA1 and 61 W/m^2 for NRA2, respectively. The RMS error is also larger for NRA2 than for NRA1. Both reanalyses however show several large spike differences, $200\text{-}300\text{ W/m}^2$, in comparison to KEO LHF during summer and autumn, related to typhoon passages.

There are various possible causes for the difference between KEO and NRA heat fluxes. One cited cause is the use of different flux algorithms for estimating the turbulent heat fluxes. Therefore, we calculated turbulent heat fluxes from NRA meteorological variables using the same bulk algorithm used for computing the KEO turbulent heat fluxes, i.e., the COARE3.0 bulk algorithm. We will refer to the resulting fluxes by COARE3.0 as NRA1C or NRA2C. Comparing the scatter plots between KEO and NRA1C LHF and KEO and NRA1 LHF (not shown here), it is clear that using COARE3.0 reduces LHF and the NRA biases, although the reduction in the NRA1C appears to be too great for LHF values above 200 W/m^2 . We see that the NRA1 LHF RMS error is not largely reduced, while the NRA2 RMS error has a large reduction (from 62 W/m^2 to 43 W/m^2). It is concluded that the LHF appears to be quite sensitive to differences in the bulk algorithm.

In order to identify further causes for the discrepancies in fluxes, we compare meteorological variables observed by KEO with reanalysis. All meteorological data of both reanalyses and KEO sensor were adjusted to a common height using the COARE algorithm. Figure 4 shows the time variation of each meteorological variable and the difference from KEO data. Since the SST and air temperature variations are quite similar to that of saturated specific humidity (Q_s) and specific humidity (Q_a), respectively, the temperature comparisons are not shown here. As expected, there exists significant seasonal variability in all variables. While wind speeds are large in winter and small in summer,

other variables are vice

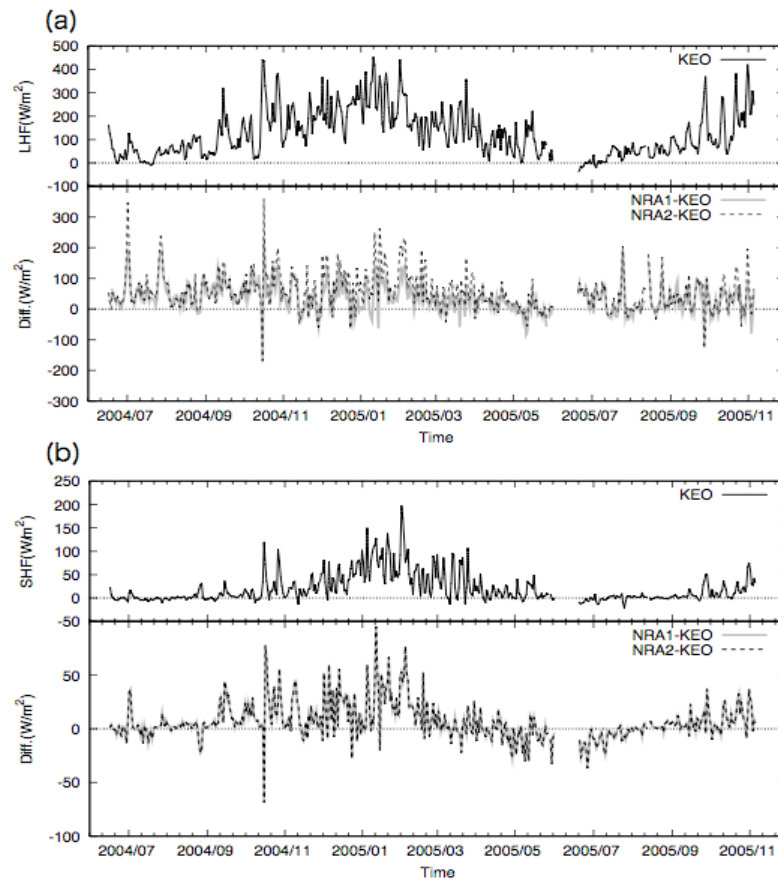


Figure 3. Same as Fig.1, except for (a) latent heat flux (LHF) and (b) Sensible heat flux (SHF).

In order to identify further causes for the discrepancies in fluxes, we compare meteorological variables observed by KEO with reanalysis. All meteorological data of both reanalyses and KEO sensor were adjusted to a common height using the COARE algorithm. Because the meteorological variable in the reanalysis is not an average value but rather an instantaneous value every 6-hours, we resample KEO data every 6-hour for comparison with the reanalyses' meteorological values.

Figure 4 shows the time variation of each meteorological variable and the difference from KEO data. Since the SST and air temperature variations are quite similar to that of saturated specific humidity (Q_s) and specific humidity (Q_a), respectively, the temperature comparisons are not shown here. As expected, there exists significant seasonal variability in all variables. While wind speeds are large in winter and small in summer, other variables are vice versa. It should be noted that winds are considerably weaker in summer of 2005 than 2004. Kako and Kubota (2006) point out that the increase of heat transfer from the atmosphere to the ocean related to the weak winds contribute to the shallow ocean mixed layer in winter of 2005-2006.

As shown in Fig.4, in comparison to the KEO, NRA1 underestimate wind speeds and NRA2, particularly during winter, overestimate wind speeds. It is interesting that NRA1 overestimates turbulent heat fluxes compared with KEO fluxes in spite of the underestimation of wind speeds. It is difficult to accurately evaluate the contribution of each meteorological variable to the flux error because the bulk formula is nonlinear. Therefore, following Jiang *et al.* [2005] and Tomita and Kubota [2006] we use daily-averaged meteorological variables from the KEO buoy, systematically substituting one component parameter with that from NRA1 and NRA2 (these data sets are hereafter referred to as substitute data sets). Of all the variables, Q_a contributes the largest error to the turbulent heat flux, consistent with the results found by Sun *et al.* [2003], Jiang *et al.* [2005], and Tomita and Kubota [2006]. For NRA1,

errors in Q_a contribute 42 W/m^2 to the RMS error in LHF. Although Q_a contributes the most to the bias in the turbulent heat flux, it is small compared with the bias caused by the algorithm errors as shown earlier.

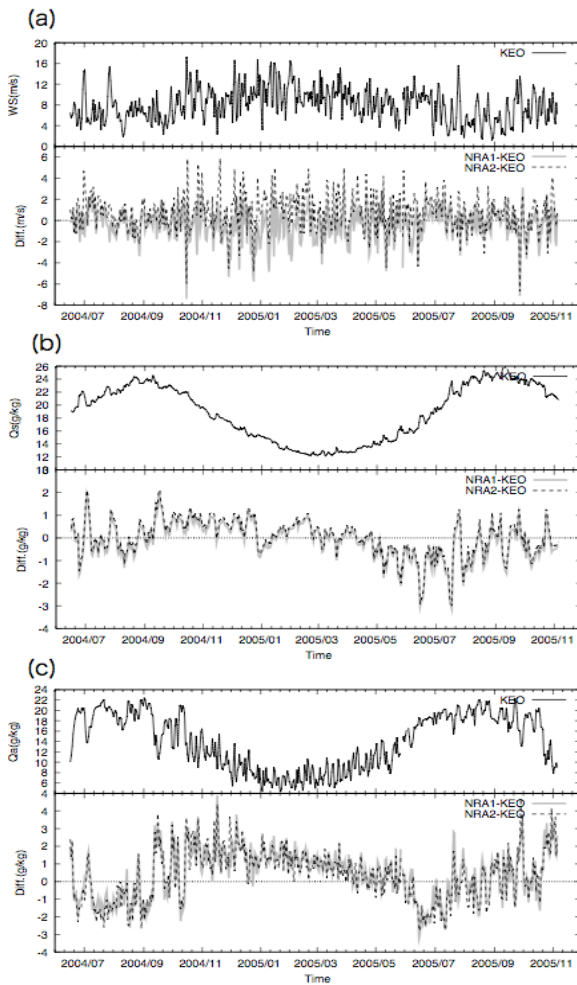


Figure 4. Same as Fig.1, except for (a) Wind speed, (b) saturated specific humidity and (c) specific humidity.

3-4. Total heat flux

Figure 5 shows time variation of total heat flux observed by KEO buoy and the difference between KEO and reanalysis total heat flux. Heat transfer from the ocean to the atmosphere occurs roughly from October to May. Clearly a huge amount of heat energy is released from the ocean to the atmosphere. In particular, the heat transfer reaches to more than 500 W/m^2 in winter, while the heat gain in summer is at most 200 W/m^2 . The differences in the total heat flux were relatively large throughout the record, except during spring 2005, when the net surface heat flux was also small. The large differences in winter are due to the large differences of LHF and SHF, while those in summer are due to the large differences in SWR shown in Fig. 1, rather than LHF and SHF. As shown in Table 1, the bias of THF strongly depends on that of LHF, while the RMS error of THF is related to both SWR and LHF.

Since the differences between KEO and reanalysis THF are mostly positive, both of the reanalyses overestimate the heat transfer from the ocean to the atmosphere. If reanalysis heat flux is used for driving a numerical ocean general circulation model, the resulting ocean would be too cool, unless other processes such as advection or mixing had compensating errors. This is a serious problem for climate research because of the unrealistic dynamical balance.

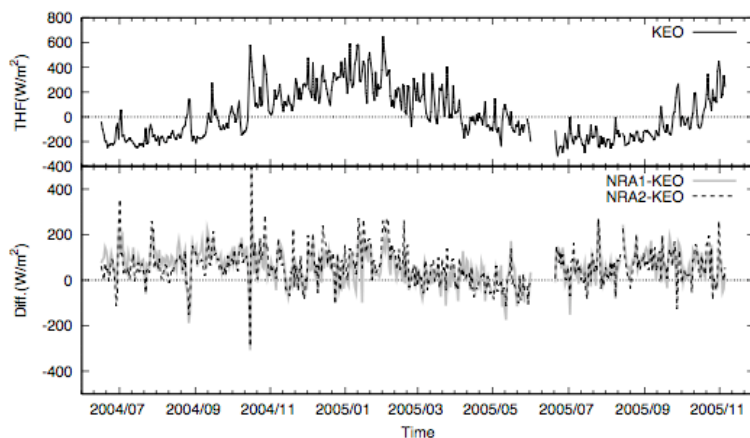


Figure 5. Same as Fig.1, except total heat flux.

4. SUMMARY

Surface heat fluxes from the Kuroshio Extension Observatory (KEO) buoy are compared with surface heat fluxes from the National Centers for Environmental Prediction (NCEP)/National Center for Atmospheric Research reanalysis (NRA1) and NCEP/Department of Energy reanalysis (NRA2). KEO surface measurements include downward solar and longwave radiation, wind speed and direction, relative humidity, rain rate, and air and sea surface temperature. For solar radiation, NRA2 had better agreement with KEO than NRA1. Both reanalyses underestimate shortwave radiation in summer and slightly overestimated it in winter. Turbulent surface heat fluxes are estimated with the KEO surface data using the Coupled Ocean-Atmosphere Response Experiment (COARE) version 3.0 bulk algorithm. Both NRA1 and NRA2 latent heat flux (LHF) are larger than KEO LHF, consistent with previous studies. However, the comparison shows larger errors than previously thought. Indeed, the latent heat flux bias for NRA1 is 41 W m^{-2} and for NRA2, 62 W m^{-2} (indicating that the bias between NRA1 and NRA2 is 21 W m^{-2}). For latent heat flux, the large bias is caused primarily by the NRA bulk flux algorithm, while the Root Mean Square (RMS) error is caused primarily by errors in the NRA meteorological variables. The combination of the biases for each heat flux is such that total NRA heat transfer from the ocean to the atmosphere is considerably larger than observed by KEO. These results highlight the importance of maintaining in situ observations for monitoring surface heat fluxes in the Kuroshio/Kuroshio Extension regions.

ACKNOWLEDGEMENT:

This research was funded by Japan Aerospace Exploration Agency.

REFERENCES:

- Chou, S. H., E. Nelkin, J. Ardizzone, R. M. Atlas, and C. L. Shie ,2003: Surface turbulent heat and momentum fluxes over global oceans based on the Goddard Satellite retrievals, version 2 (GSSTF2), *J. Climate*, **16**, 3256–3273.
- Cronin, M. F., C. W. Fairall, and M. J. McPhaden ,2006: An assessment of buoy derived and NWP surface heat fluxes in the tropical Pacific, *J. Geophys. Res.*, in press.
- Fairall, C. W., E. F. Bradley, J. E. Hare, A. A. Grachev, and J. B. Edson,2003: Bulk parameterization of air-sea fluxes: Updates and verification for the COARE algorithm, *J. Climate*, **16**, 571–591.
- Jiang, C. L., M. F. Cronin, K. A. Kelly, and L. Thompson,2005: Evaluation of a hybrid satellite- and NWP-based turbulent heat flux product using Tropical Atmosphere-Ocean (TAO) buoys, *J. Geophys. Res.*, **110**, C09007, doi:10.1029/2004JC002824.
- Kalnay, E. M. et al.,1996: The NCEP/NCAR 40-year reanalysis project, *Bull. Am. Meteorol. Soc.*, **77**, 437–471, 1996.
- Kanamitsu, M., W. Ebisuzaki, J. Woollen, P. Potter, and M. Fiorion,2000: An overview of NCEP/DOE reanalysis-2, a per represented at Second WCRP International Conference on Reanalysis, World Meteorol. Org., Reading, UK.
- Kubota, M. , N. Iwasaka , S. Kizu , M. Konda, and K. Kutsuwada,2002: Japanese Ocean Flux Data Sets with Use of Remote Sensing Observations (J-OFURO), *J. Oceanogr.*, **58**, 213–225.
- McPhaden, M. J. et al.,1998: The Tropical Ocean Global Atmosphere (TOGA) observing system: A decade of progress, *J. Geophys. Res.*, **103**, 14,169–14,240.
- Moore, G. W. K., and I. A. Renfrew,2002: An assessment of the surface turbulent heat fluxes from the NCEP-NCAR reanalysis over the western boundary currents, *J. Climate*, **15**, 2020–2037.
- Sun, B., L. Yu, and R. A. Weller,2003: Comparison of surface meteorology and turbulent heat fluxes over the Atlantic NWP model analyses versus moored buoy observations, *J. Climate*, **16**, 679–695.
- Tomita, H., and M. Kubota,2006: An analysis of the accuracy of Japanese¥ Ocean Flux data sets with Use of Remote Sensing Observations (J-OFURO) satellite-derived latent heat flux using moored buoy data, *J. Geophys. Res.*, **111**, C07007, doi:10.1029/2005JC003013.